WWJMRD 2022; 8(06): 14-28
www.wwjmrd.com
International Journal
Peer Reviewed Journal
Refereed Journal
Indexed Journal
Impact Factor SJIF 2017: 5.182 2018: 5.51, (ISI) 2020-2021: 1.361
E-ISSN: 2454-6615

Bassey, Bassey Okon
Department of Mechanical Engineering, Akwa Ibom State University, Nigeria.

Correspondence:
Bassey, Bassey Okon
Department of Mechanical Engineering, Akwa Ibom State University, Nigeria.

Thermal performance and functional sustainability limit of working fluids in a low-heat regenerative organic Rankine cycle at varying evaporator heat input

Bassey, Bassey Okon

Abstract
Thermal and functional sustainability limit (FSL) or exergetic sustainability limit (ESL) of refrigerants in a regenerative organic Rankine cycle (RORC) is presented. The objective is to determine the limit where a particular refrigerant can be more eco-friendly at some thermodynamic inputs. Three refrigerants R113, R141b and R245fa were considered at different evaporator heat inputs (EHI). The FSL for the refrigerants were calculated at 1.10 for 247.92 kW, 0.92 for 191.88 kW and 1.025 for 240.11kW using R245fa, R113 and R141b respectively. Also, the environmental effect factor (EEF) at FSLs of the refrigerants were estimated at 0.00958, 0.01076 and 0.00958 in the same order. The environmental damage at EHI range between $180 \leq EHI \leq 320$kW was 0.35 % for R245fa, 12.25 % for R113 and 0.991 % for R141b. R245fa was more sustainable than other refrigerants. However, comparing the thermodynamic approximated values of the refrigerants with the ODP and GWP classifications the two were reasonably associated. Conversely, the study concluded that refrigerants have a limit of optimal performance where they function with less environmental impact. The latter is described as the functional sustainability limit. Thus, the design and optimisation of systems to operate on such optimal limits will enhance performance and reduce environmental complications.

Keywords: Thermal, functional sustainability, regenerative, evaporator, exergy.

1.0 Introduction
The steady increase in the cost of conventional energy resources and associated environmental concerns in recent times have made the utilisation of low temperature waste heat attractive. The organic Rankine cycle (ORC) among other cycles such as supercritical Rankine cycle (SRC), Kalina cycle, Goswami cycle and trilateral flash cycles are the most common cycles in the utilization of low temperature waste heat [1-5]. The ORC offers a wider prospect to operate at low temperatures, making it possible to generate electricity from different energy sources such as solar, geothermal, waste heat and biomass, etc.[6-9]. However, the non-hybrid form of ORC is simple, low maintenance cost and high recovery efficiency [10]. For these reasons, many scholars have presented different studies vis-à-vis the organic Rankine cycles. For instance, [11, 12] studied the impacts of thermodynamic variables on the performance of ORC with different refrigerants. The thermodynamic variables for each refrigerant were optimised with the exergy efficiency. Additionally, the refrigerants were identified based on the saturation vapour curves and their responses to the heat source temperature. Their results show that proper selection of working fluid is an important criterion for determining system performance. Similarly, [13] investigated the performance of a transcritical organic Rankine cycle with and without internal heat exchanger for different refrigerants. Better performance was obtained with supercritical cycles than the subcritical cycles. The reason was ascribed to improved thermal match existing between the sensible heat source and the working fluid. In the same vein [14]

examined the performance of ORC with superheating for different organic working fluids. The study indicated that for a specified heat source temperature both the energy and exergy efficiencies might exist at peak value or increase monotonically with the evaporating temperature. Further works of [15] measured the performance of ORC with R 123, PF 5050 and n-pentane refrigerants for a geothermal plant. The influence of condensation and evaporation temperatures were studied for different cooling water velocities. Also, [16] investigated the thermodynamic performance of thirty-one refrigerants involving sub-critical and supercritical ORCs applied to a geothermal system. Their deduction shows that system performance is absolutely dependent on refrigerant thermodynamic properties and operating conditions. Studies on ORC inputs variables and variations such as evaporator pressure, evaporator temperature, heat source temperature, pitch point temperature and condensation temperature are sufficiently discussed in regards to ORC performance. The thermodynamic performance of transcritical ORC under varying heat source temperature was investigated by [17]. The studies established that the cycle efficiency increases for increasing source temperature (ST) and at fixed ST, the peak value exist in the supercritical region. Furthermore, [18] analysed different ORC configurations with different refrigerants and at varying heat source temperature. The results indicate R-123 gave better performance and less irreversibility for all the ORC configurations. The influence of variable heat addition on the heat transfer behaviour was investigated in [19] and the findings show high refrigerant heat transfer coefficient at full load from the diesel engine. Other studies include [20] who considered the heat transfer ability of R245fa and exergy loss distribution in a subcritical ORC. The critical input values like heat source temperature, pitch point temperature, the isentropic efficiency of the expander and cooling water temperature were studied. On the same note [21] examined the effect of evaporator pressure, the pitch point temperature difference (PPTD) on ORC performance using R245fa, R123, R142b, Isobutene, R113, and R141b. The study indicated an increase in ORC performance for all working fluid at small values of PPTD. Nevertheless, the survey literature above has extensively covered refrigerants performance for different inputs conditions with less emphasis on the refrigerant functional sustainability limit or exergetic-sustainability limit. The latter has not be published in the open domain. Consequently, the present study categorises refrigerants to have a functional sustainability limit irrespective of the ODP (ozone depleting potential). The functional sustainability limit (FSL) defined in this study is a limit where the impact of the working fluid on the environment is minimum at some thermodynamic inputs. Though, related studies based on evaporator pressure input on the environmental sustainability of ORCs is contained in [22]. Performance of different ORCs was considered, and the most sustainable system and refrigerant were identified based on the exergetic sustainability indicators. The present study, therefore, differs in that it is intended at approximating the sustainability limit of working fluids in a regenerative organic Rankine cycle (RORC) at varying evaporator heat input (EHI). The contribution of this study will specifically provide a logical basis for system design as to how effectively a working fluid can be utilized. Also, the study will establish the method for determining the environmental safe operating limit of working fluids which is not highlighted in open literature.

2.0 ORCs description and thermodynamic modelling

The RORC system is presented in Fig.1a while Fig.1b depicts the temperature-entropy diagram of the RORC. The system (Fig.1a) consists of the following: the evaporator, internal heat exchanger (IHE) condenser, expander and the pump. The refrigerant is supplied to the evaporator at state (5) by the pump where it absorbed heat from the heat source to become vapour. The vapour exits from the evaporator at high pressure into the turbine where the enthalpy of the vapour is converted into useful work by the turbine. After expansion, the vapour at low-pressure exit the turbine through the state (8) into the condenser where it condenses into a saturated liquid at high pressure. The liquid is pumped into the internal heat exchanger at (state 3) and then to the FWH where the liquid is completely subcooled and is pumped to the evaporator to commence the cycle.

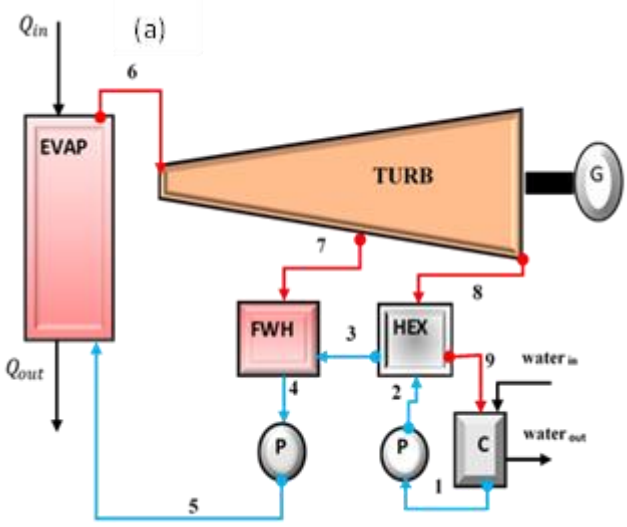

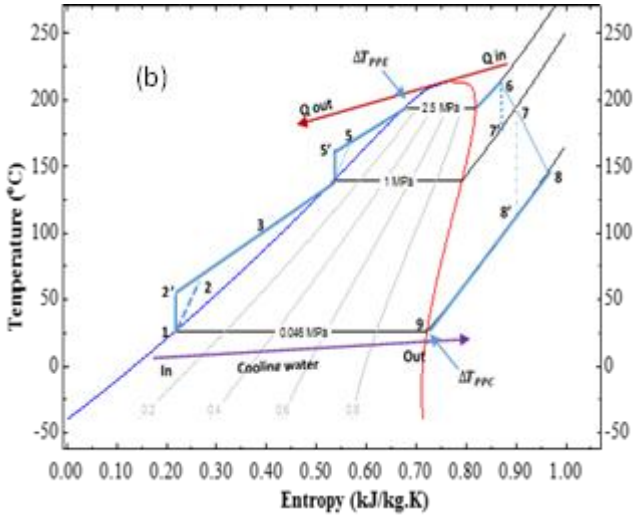

Fig. 1. Representations of (a) Regenerative organic Rankine cycle, (b) Temperature-Entropy diagram.

2.1 Thermodynamic assumptions

The following broad assumptions are considered in this parametric analysis: The components of the RORC system operates in a steady state condition. The potential and kinetic energies plus the heat losses are ignored. The pump and the isentropic turbine efficiencies are set at 90 and 85%, respectively. The inlet temperature of water to the condenser, the evaporator and the heat input conditions are approximated at 298 K, 2.5 MPa and 252 kW respectively. Furthermore, the ambient conditions are taken at 25 °C and 101.325 kPa. The refrigerants used in this study included R245fa, R141b and R113. The properties of these refrigerants are presented in Table 1.

Table 1: Property of refrigerants [23, 24].

S/N	Property	R113	R141b	R245fa
1	Chemical formula	$Cl_2FC\text{-}CCF_2$	$CH_3CCl_2F_2$	$CF_3CH_2CHF_2$
2	Molecular mass (g/mol)	187.37	116.95	134
3	Normal boiling point (^{O}C)	47.6	32.05	15.3
4	Critical temperature (^{O}C)	214.1	204.5	154.05
5	Critical pressure (Mpa)	3.39	4.25	3.64
6	Liquid phase density (kg/m^3) (1 atm)	1508	1220	1339
7	GWP (kg CO_2)	6130	725	950
8	ODP	1.0	0.11	0.0

2.2 Thermodynamic modelling

The steady-state exergy flow equation per unit mass for a thermal process is expressed in [25].

$$\dot{I} = \sum_{in} \dot{m}_e - \sum_{out} \dot{m}_e - \dot{E}_{in}^{Q} - \dot{E}_{out}^{W} = T_0 \dot{S}_{gen} \quad (1)$$

Where $\dot{I}$, $\dot{m}_e$, $\dot{E}_{in}^{Q}$ and $\dot{E}_{out}^{W}$ are rate of exergy destruction, mass flow rate, heat and work transfer quantities while $\dot{S}_{gen}$ is the entropy generation respectively. The thermodynamic equation describing the thermo-mechanical component of exergy flow in specific terms for a thermodynamic process is stated [25] as:

$$e_x = [h - h_0] - T_0(s - s_0) \quad (2)$$

Where h_0, and s_0 denotes specific enthalpy and specific entropy at ambient state P_0 *and* T_0, respectively. Furthermore, the common mathematical equation for entropy generation in a steady state condition is defined by [26]

$$\sum \frac{Q_k}{T_k} + \sum \dot{m}_e s_e + \sum \dot{m}_i s_i + \dot{s}_{gen} = \frac{ds_{cv}}{dt} \quad (3)$$

$$\sum \frac{Q_k}{T_k} - \sum \dot{m}_e s_e + \sum \dot{m}_i s_i + \dot{s}_{gen} = \frac{ds_{cv}}{dt} \quad (4)$$

For steady state condition $\frac{ds_{cv}}{dt}$ diminishes thus

$$\dot{s}_{gen} = \sum \dot{m}_e s_e - \sum \dot{m}_i s_i - \sum \frac{\dot{Q}_k}{T_k} \quad (5)$$

T_k, and $\dot{Q}_k$ are the heat source and heat transfer rate respectively. The expression for the chemical exergy of refrigerants is defined in [27] as,

$$e_{ch} = \frac{e_{ch}^0}{M}\left[\frac{T_0}{298.15}\right] + \frac{\Delta H_0}{M}\left[\frac{T_0 - 298.15}{298.15}\right] \quad (6)$$

2.2.1 Exergy balance in the RORC components

Eqs. (1) and (2) are applied in (Fig. 1a) to describe the exergy distribution rate in the components of the RORC

Pump 1 (1-2), $\dot{E}x_1 + \dot{w}_{pum1} = \dot{E}x_2 + \dot{E}_{Dpum1}$ (7)

Pump 2 (4-5), $\dot{E}x_4 + \dot{w}_{pum2} = \dot{E}x_5 + \dot{E}_{Dpum2}$ (8)

Evaporator (4-5) $\dot{E}x_5 + \left(1 - \frac{T_0}{T_{in}}\right) Q_{in} = \dot{E}x_6 + \dot{E}_{Deva}$ (9)

Turbine (6-7 &6-8), $\dot{E}x_6 = \dot{E}x_8 + \dot{E}x_9 + \dot{w}_{tub} + \dot{E}_{Dtub}$ (10)

Heat exchanger (2-3&8-9), $\dot{E}x_8 + \dot{E}x_2 = \dot{E}x_9 + \dot{E}x_3 + \dot{E}_{Dhe}$ (11)

Feedwater heater (7-4-3), $\dot{E}x_7 + \dot{E}x_3 = \dot{E}x_4 + \dot{E}_{DFwh}$ (12)

Condenser (9-1), $\dot{E}x_9 = \dot{E}x_1 + \dot{E}_{Dcon}$ (13)

The total exergy destruction (D_{total}) and the overall exergy efficiency ($\psi_{overall}$) are expressed in Eqs. (14) and (15) respectively.

$$D_{total} = D_{Pum1} + D_{he} + D_{fwh} + D_{Pum2} + D_{eva} + D_{tub} + D_{con} \quad (14)$$

$$\psi_{overall} = \frac{\dot{W}_{tub} - (\dot{W}_{pum1} + (\dot{W}_{pum2})}{\left(1 - \frac{T_0}{T_{in}}\right) Q_{in}} \quad (15)$$

The effectiveness ϵ of the feed water heater regarding exergetic streams can be expressed in Eq. (16) While the components entropy and exergy efficiency balances are depicted in Table 2

$$\epsilon = \frac{m_3 \left\| c_p[T_3 - T_0] - T_0\left\{c_p \ln\left[\frac{T_3}{T_0}\right] - R \ln\left[\frac{P_3}{P_0}\right]\right\}\right\|}{m_6 \left\| c_p[T_6 - T_0] - T_0\left\{c_p \ln\left[\frac{T_6}{T_0}\right] - R \ln\left[\frac{P_6}{P_0}\right]\right\}\right\| + m_2 \left\| c_p[T_2 - T_0] - T_0\left\{c_p \ln\left[\frac{T_2}{T_0}\right] - R \ln\left[\frac{P_2}{P_0}\right]\right\}\right\|} \quad (16)$$

Table 2: Components entropy and exergy efficiency balances for the RORC.

Component	Entropy balance	Component exergy efficiency
Pump 1	$s_1 - s_2 + s_{gen}, pum1 = \frac{Q_{Pum1}}{T_0}$	$\psi_{pum1} = \frac{\dot{E}x_2 - \dot{E}x_1}{(\dot{w}_{pum1})}$
Pump 2	$s_4 - s_5 + s_{gen}, pum2 = \frac{Q_{Pum2}}{T_0}$	$\psi_{pum2} = \frac{\dot{E}x_5 - \dot{E}x_4}{(\dot{w}_{pum2})}$
Evaporator	$s_5 - s_6 + s_{gen}, eva = \frac{Q_{eva}}{T_0}$	$\psi_{eva} = \frac{\dot{E}x_6}{\left[1 - \frac{T_0}{T_Q}\right] Q_{in} + \dot{E}x_5}$
Turbine	$s_6 - s_7 + s_8 + s_{gen}, tub = \frac{Q_{tub}}{T_0}$	$\psi_{tub} = \frac{\dot{w}_{tub}}{\dot{E}x_6 - \dot{E}x_7 - \dot{E}x_8}$
Heat exchanger	$s_8 + s_2 - s_3 - s_9 + s_{gen}, he = \frac{Q_{he}}{T_0}$	$\psi_{he} = \frac{\dot{E}x_3 - \dot{E}x_2}{\dot{E}x_3 - \dot{E}x_9}$
Feed water heater	$s_7 + s_3 - s_4 - s_9 + s_{gen}, fwh = \frac{Q_{fwh}}{T_0}$	$\psi_{fwh} = \frac{\dot{E}x_4}{\dot{E}x_7 + \dot{E}x_3}$
Condenser	$s_9 - s_1 + s_{gen}, con = \frac{Q_{con}}{T_0}$	$\psi_{con} = \frac{\dot{E}x_9 - \dot{E}x_1}{\dot{E}x_9}$

3.0 Exergy-based sustainability indicators

The exergetic-sustainability indicators are defined for the ORC in (Fig. 1a) based on the exergy balance at the different state point.

3.1 Waste *exergy ratio (WER)*

In a thermal system undergoing thermodynamic processes, exergy destruction (ED) exists within the system boundary due to pressure change. Equally, exergy is lost to the environment due to the interaction between the system and the environment. The overall waste exergy is thus calculated as the summation of the destroyed exergy in the system components and lost exergy to the environment [28].

$$\sum Ex_{we,out} = \sum \dot{E}x_{dest,out} + \sum \dot{E}x_{loss,out} \quad (17)$$

Furthermore, for the RORC system in (Fig.1a) the exergy destruction within the process boundary dominates on the assumption that the exergy loss to the environment is very insignificant. Thus, the overall waste exergy is equal to the total exergy destruction in the system components. Subsequently, Eq. (17) reduces.

$$\sum \dot{E}_{xwaste} = \sum \dot{E}_{x\ destroyed} \quad (18)$$

The waste exergy ratio (WER) is defined as the ratio of the total waste exergy to the total input exergy [28].

$$WER = \frac{\text{Total waste exergy}}{\text{Total input exergy}} = \frac{\sum \dot{E}x_{waste}}{\sum \dot{E}x_{input}} = \frac{\sum \dot{E}x_{destroyed}}{\sum \dot{E}x_{input}} \quad (19)$$

3.2 *Environmental effect factor* (EEF)

The environmental effect factor (EEF) is a major environmental sustainability indicator. It specifies the extent of damage caused by a thermodynamic system to the environment owing to the waste exergy destruction and output [28].

$$EEF = \frac{\text{Waste exergy ratio}}{\text{Exergy efficiency}} = \frac{\dot{E}x_{waste}}{\psi} = \frac{\dot{E}x_{dest.}}{\psi} \quad (20)$$

Additionally, Eq. (20) can be applied to an RORC system like that considered in (Fig.1a). In practice there exist material interaction with the environment despite the defined structure of the ORC system. Thus, on this supposition Eq. (20) is applied in (Fig. 1a) to determine the environmental damage caused by the working fluid used for heat transfer in the RORC.

3.3 *Exergy destruction factor (EDF)*

The exergy destruction factor (EDF) indicates the decrease of the positive effect of the system exergetic sustainability indicators. EDF is calculated as the ratio of exergy destruction to the overall exergy input which ranges from 1 to 0 [29].

$$EDF = \frac{\dot{E}x_{dest}}{\dot{E}x_{in}}, (0 \le EDF \le 1) \quad (21)$$

For the considered system in (Fig. 1a) the EDF will be calculate for each value of EHI for the entire considered range of EHI.

3.4 Exergetic sustainability index (ESI)

The exergetic sustainability index (ESI) delineates the degree of sustainability of a system with the environment. It is defined as the reciprocal of the EEF. The ESI range is between 1and ∞. The higher system efficiency connotes low WER, EEF and higher ESI [28, 30].

$$ESI = \frac{1}{EEF}, (0 \le ESI \le \infty) \quad (22)$$

4.0 Functional sustainability limit or Exergetic sustainability limit

The term functional sustainability limit (FSL) or exergetic sustainability limit (ESL) is defined in this study as a limit where the impact of the system on the environment is minimum at some thermodynamic inputs. In evaluating the FSL, the environmentally safe limit (ESAL) is first determined in the EEF curve for a particular evaporator heat input (EHI). For example, if the relationship between EEF and EHI is defined by the polynomial in Eq. (23) as,

$$Y = A + BX + CX^2 \quad (23)$$

Where Y represents the environmental impact factor (EEF), A, B and C are constants and X is the evaporator heat input (EHI). At minimum $\left(\frac{\partial Y}{\partial X} = 0\right)$, the X (EHI) and Y (EEF) values are determined (Fig.2a). This minimum point at coordinates (Y (EEF), X (EHI)) is called the environmentally safe limit (ESAL) while region ABCD is the environmentally safe operating region (Fig.2a). Furthermore, to determine the FSL or the ESL the X (EHI) value obtained at minimum $\left(\frac{\partial Y}{\partial X} = 0\right)$ is estimated in the exergetic sustainability index (ESI) curve (Fig.2b). At this point the value of the ESI on the curve is obtained at coordinates (X (EHI), ESI) which defines the FSL or ESL. Beyond this limit of X (EHI) the sustainability of the system decreases. The area ABCD in (Fig.2b) is the region of best refrigerant performance. Values of EHI chosen within this region will have less environmental impact for the particular working fluid. Additionally, values of FSL will vary for different working fluids and cycle configurations. The term FSL is refer to be the same as exergetic sustainability limit (ESL).

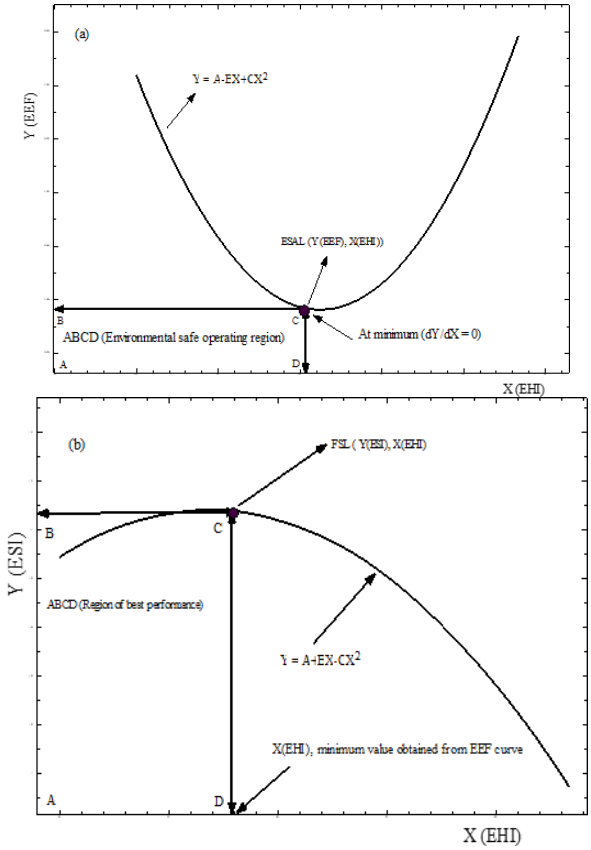

Fig. **2**. Description of thermodynamic regions and limits (a) ESAL and (b) ESL in a regenerative ORC.

5.0 Results and Discussion

5.1 Thermal performance of the RORC

The results of the thermal performance of a regenerative organic Rankine cycle is presented. Three different working fluids were considered, R113, R141b and R245fa. Moreover, the thermodynamic flow parameters for the refrigerants at different state points are presented in Table 3. The initial operating pressure conditions with R113, R141b and R245fa are set at 0.046 MPa, 0.0793MPa and 0.1066MPa respectively. The entropy generation for the different working fluids is also presented in Table 3 which is higher for R141b than other refrigerants.The effect of the EIH was considered for all the performance indicators, like overall exergy efficiency (OEE), overall exergy destruction (OED) and turbine output (TOP) Fig. 3 (a-c). From Fig.3a the OEE varies from 45.64 to 49.24 % for EHI range between 180 and 320 kW. However, the OEE increases initially from 180 kW for all the refrigerants and attain a common efficiency of 47.82 % at EHI of 206 kW. Above 206 kW of EHI, the OEE with R113 decreases for all variations in EHI while OEE increases steadily with R141b and R245fa to about 261 kW. Additionally, the OED and the TOP with all refrigerants increases with increasing EHI (Fig.3b and 3c). The reason for the increase in OED (Fig. 3b) is apparent since at fixed evaporator pressure the difference between the temperature of the hot gas and that of the evaporator is large. Subsequently, the latter results in large entropy generation and thus increase in the cycle OED. Nevertheless, the exergy destruction obtained with R141b is the lowest (Fig. 3b) with maximum TOP of nearly 76 kW archived at 320 kW EHI (Fig. 3b).The effect of EHI on component exergy destruction (CED) and the component exergy efficiency (CEF) is depicted in Figures 4 and 5. The CED (Fig. 4a-4c) is dominated by the condenser and the evaporator for all the refrigerants. On the other hand, the CED varies differently with EHI for the respective refrigerants. For example, in Fig.4a and Fig.4b, the exergy destruction (ED) of the condenser decreases with increasing EHI while in Fig.4c the ED of the condenser increases with increasing ED using R245fa. Similarly, the ED of the evaporator in Fig.4c decreases with increasing EHI while others show the reverse. The variations in the CED is dependent on the refrigerant thermodynamic properties and the state operating conditions. Furthermore, the average ED for instance in the evaporator for EHI ranged between $180 \leq EHI \leq 320kW$ was not greater than 20.83 kW, for R113, 26 kW, for R113 and 13.09 kW, for R245fa. The low values of ED obtained with R245fa suggest that R245fa has considerable environmental sustainability [22]. The CEF for R113, R141b and R245fa are depicted in Figs. 5a to 5c. Component efficiencies are high with R245fa than R113 and R141b. On the overall cycle performance, R141b has the highest efficiency for the EHI range between$180 \leq EHI \leq 320kW$.

Table 3: Thermodynamic flow parameters for the ORC at different state points.

Point	Energy [kJ/kg]	Exergy [kW]	Entropy [kJ/kg.K]	Temperature [ºC]	Pressure [Bar]
R113					
1	56.49	0.000	0.213	25.00	0.046
2	57.10	0.0007	0.215	25.67	0.046

3	71.00	0.2910	0.261	40.00	1.000
4	169.40	19.270	0.531	138.00	1.000
5	170.60	19.640	0.534	139.10	2.500
6	408.30	116.00	1.027	298.60	2.500
7	388.30	29.370	1.027	266.90	1.000
8	322.40	17.150	1.027	181.20	0.046
9	308.50	13.790	0.995	163.60	0.046
R141b					
1	67.51	0.0000	0.2541	25.00	0.079
2	68.63	0.0027	0.2579	25.98	1.470
3	86.17	0.3601	0.3149	40.00	1.470
4	213.70	25.420	0.6644	138.00	1.470
5	215.80	26.040	0.6691	139.50	3.420
6	453.50	117.00	1.1790	238.50	3.420
7	429.80	34.100	1.1790	196.00	1.470
8	348.90	3.8660	1.1790	92.02	0.079
9	331.40	1.9950	1.130	71.32	0.079
R245fa					
1	55.60	0.000	0.210	25.00	0.107
2	56.70	0.004	0.214	26.27	1.737
3	69.79	0.323	0.256	40.00	1.737
4	160.70	18.530	0.504	138.00	1.737
5	162.00	18.930	0.507	139.20	3.192
6	399.80	111.900	1.011	300.90	3.192
7	381.50	27.020	1.011	265.30	1.737
8	305.20	8.264	1.011	137.60	0.107
9	292.10	5.749	0.978	117.20	0.107

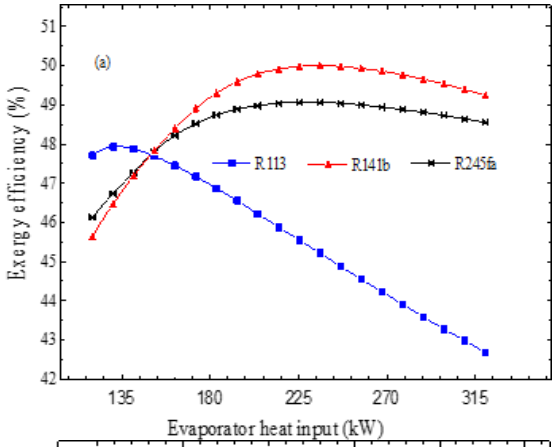

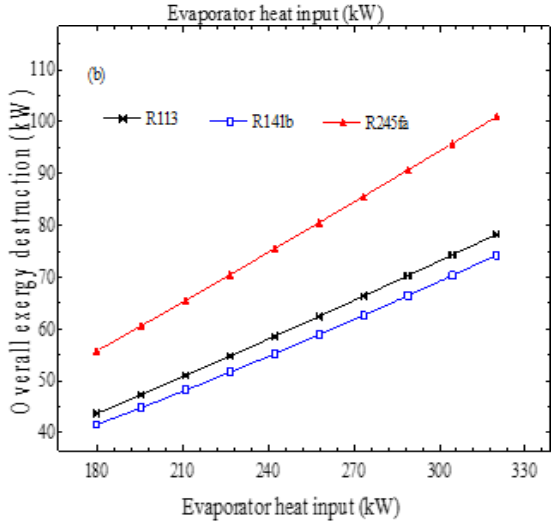

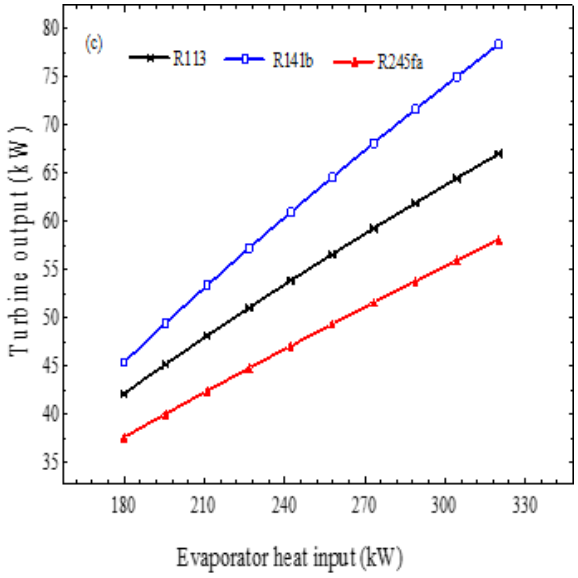

Fig. 3: Effect of EHI on (a) Overall exergy efficiency (b) Overall exergy destruction (c) Turbine power output.

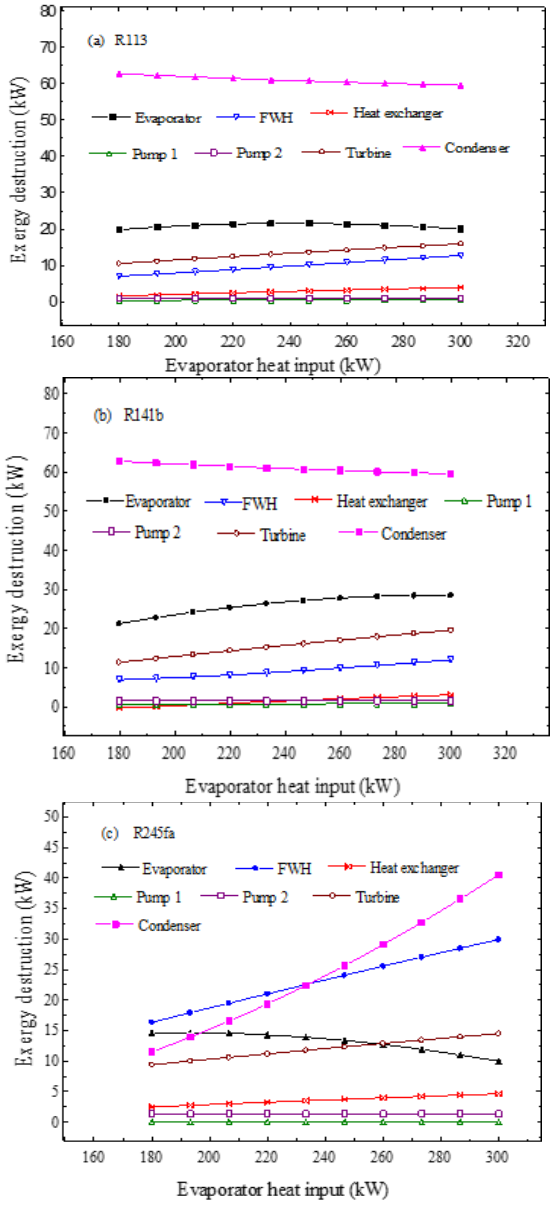

Fig. 4: Effect of EHI on component exergy destruction with (a) R113 (b) R141b (c) R245fa.

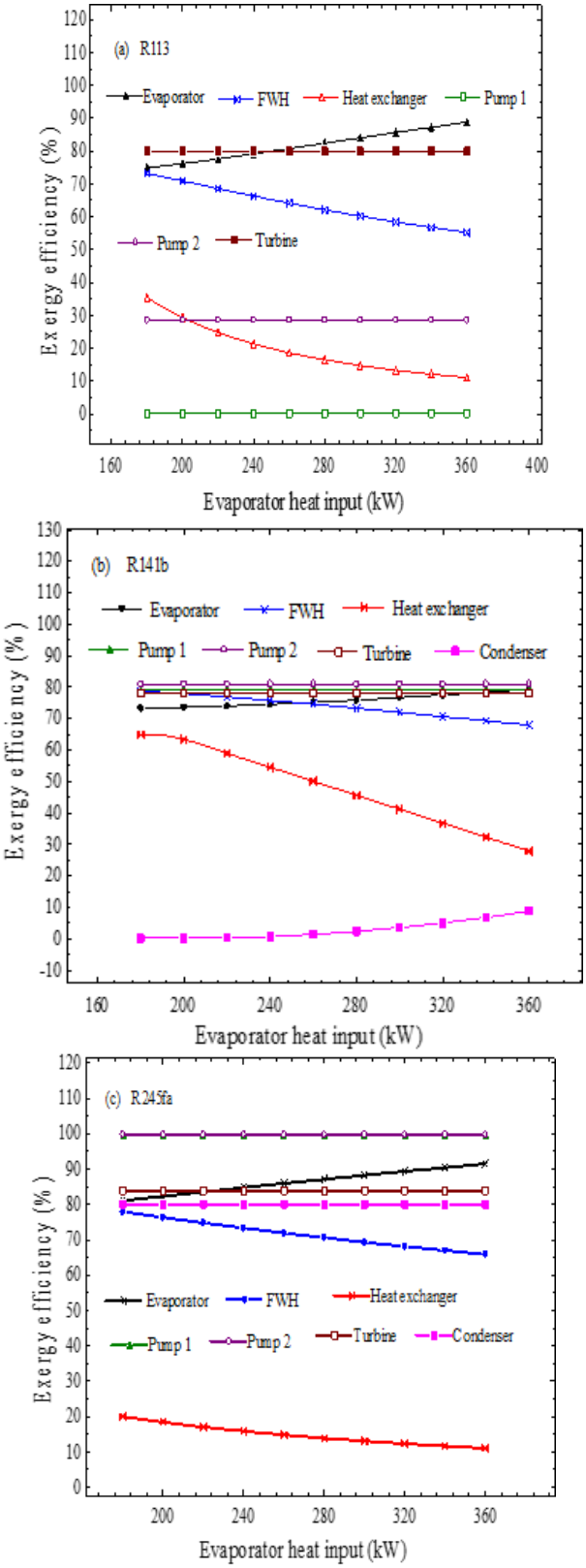

Fig. 5: Effect of EHI on component exergy efficiency with (a) R113 (b) R141b (c) R24,

5.2 *Exergetic sustainability indicators*

The exergetic sustainability indicators for the three working fluids are presented in Figs.6, 7, 8 and Tables 4-6. The effect of EHI on EEF with R245fa is shown in (Fig.6a). Maximum values of 0.009801 and 0.00985 EEF exist at EHI of 180 and 320 kW respectively with a notable increase of 0.38 % in EEF. The 0.38 % increase in EEF defines the possible environmental damage if the system is operated between 180 and 320 kW EHI. The exergetic sustainability index (which is a measure of sustainability level) decreases from 1.109 to 0.9949 (Fig.6b). Between the EHI limit of $180 \leq EHI \leq 320kW$, the ESI dropped approximately by 10.29 % which shows that the system will not be sustainable if operated at high EHI. This suggests that working fluids have a limit where they performed optimally with less environmental impact. The latter is described in this study as the functional sustainability limit or exergetic sustainability limit.

Furthermore, the WER obtained with R245fa increased steadily from 0.475 to 0.493 for all EHI ranged between $180 \leq EHI \leq 320kW$ (Fig.6c). From Eq. (18), it can be inferred for increased EHI the internal exergy destruction within the component boundary increases owing to the large temperature variance between the R245fa and the EHI temperature. This accountable for the steady increase in WER for all EHI range.The exergetic performance of the RORC with other refrigerants R113 and R141b are presented in Figs. 7(a-c) and 8(a-c) respectively. From Fig.7a, the EEF increases for all increasing EHI with a maximum value of 0.01225 obtained at EHI of 320 kW. Between the operating limits of EHI ($180 \leq EHI \leq 320kW$) the environmental impact was about 12.25 %. Additionally, the environmental impacts between R113 and R245fa were compared for extreme conditions of EHI at 180 and 320 kW. The result shows that R113 affects the environment eight times more (about 8.7 %) at EHI of 180 kW and twenty-one times more (about 21.7 %) at EHI of 320 kW than R245fa. The ESI with R113 was found to decrease with increasing EHI showing the highest ESI value of 0.96 at 180 kW and the lowest ESI value at 320 kW. Nonetheless, the WER show the same increasing trend for all increasing values of EHI. Internal exergy destruction denominates in the RORC using R113. For instance, comparing the WER for R113 and R245fa, it is observed that the internal exergy destruction using R113 is about 6.67 % higher than R245fa at 180 kW EHI, 7.12 % at 196 kW EHI and 11.03 % at 320 kW EHI. Fig.8 (a-c) depicts the exergetic indicators with R141b for EEF, ESI and WER. The R141b follows a similar trend with R245fa although the EEF values are higher than R245fa. Minimum values of EEF existed and ranged between $0.01005 \leq EEF \leq 0.00992$ for EHI range between 180 and 227 kW (Fig.8a). The environmental impacts by R141b within the operating EHI limits (180 and 320 kW) was estimated at 0.985 %. In the same vein, the WER decreases by 4.91 % between $180 \leq EHI \leq 320$ with maximum ESI attained at 1.04 (Fig.8b). The WER plot in Fig.8c differs in trend from R245fa (Fig.6c), and R113 (Fig.7c) in that WER shows a decreasing and increasing trend for varying EHI. This suggests that R141b may have a wider sustainability limit than R113.Its functional capabilities and suitability will be discussed in the succeeding section.Furthermore, the exergy destruction factor (EDF) for the three working fluids is shown in Tables 4-6 for varying EHI. The EDF values are ranged between $0 \leq EDF \leq 1$ [30] and indicate where exergy destruction dominants in a thermodynamic system with different components. From Tables 4 to 6 the EDF varies for different refrigerants and components. Lower EDF values are obtained with R245fa in some components that other refrigerants and vice versa. Additionally, low values of EDF signifies less entropy generation for a particular component which is desired. Though, the EDF is essentially a function of the thermodynamic inputs, state conditions and refrigerant thermodynamic properties.

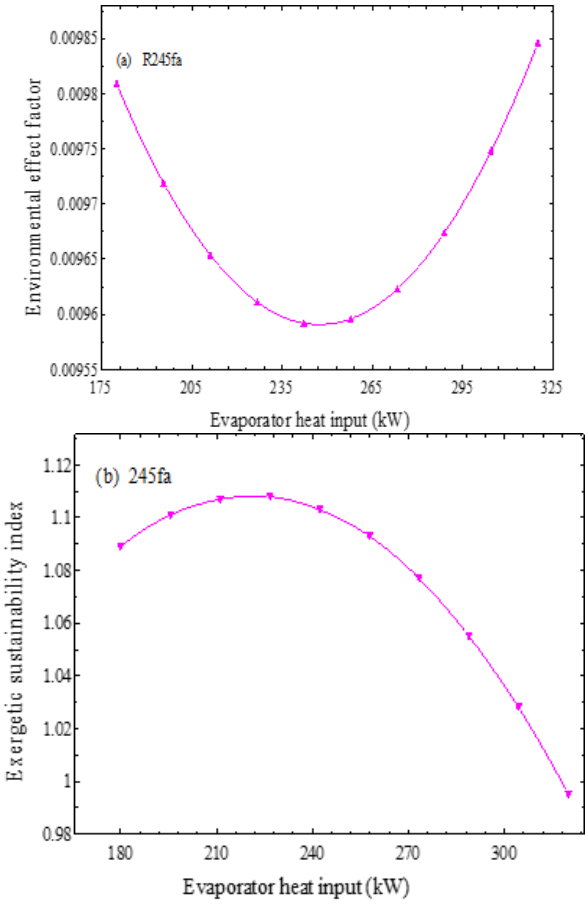

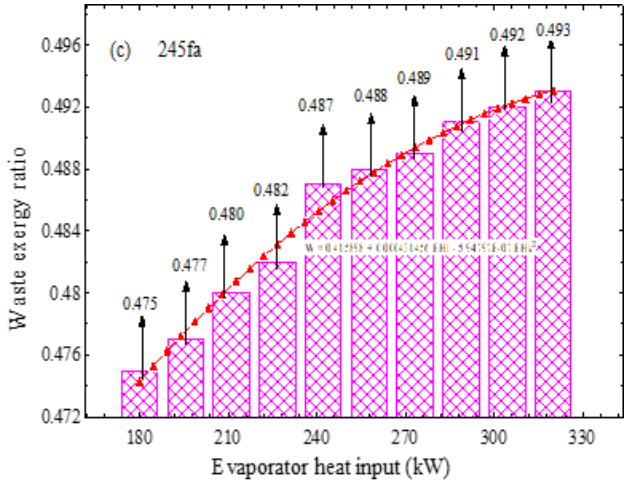

Fig. 6: Effect of EHI on (a) EEF (b) ESI and (c) WER with R245fa.

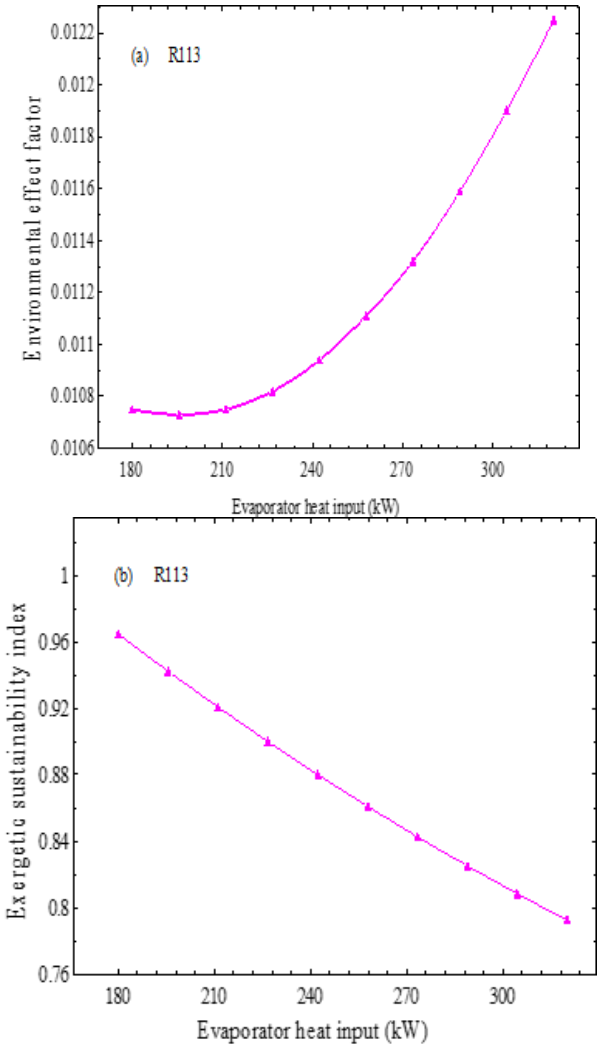

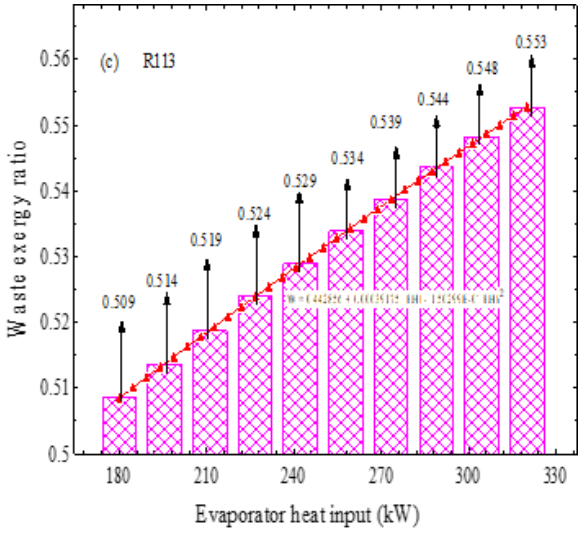

Fig. 7: Effect of EHI on (a) EEF (b) ESI and (c) WER with R113.

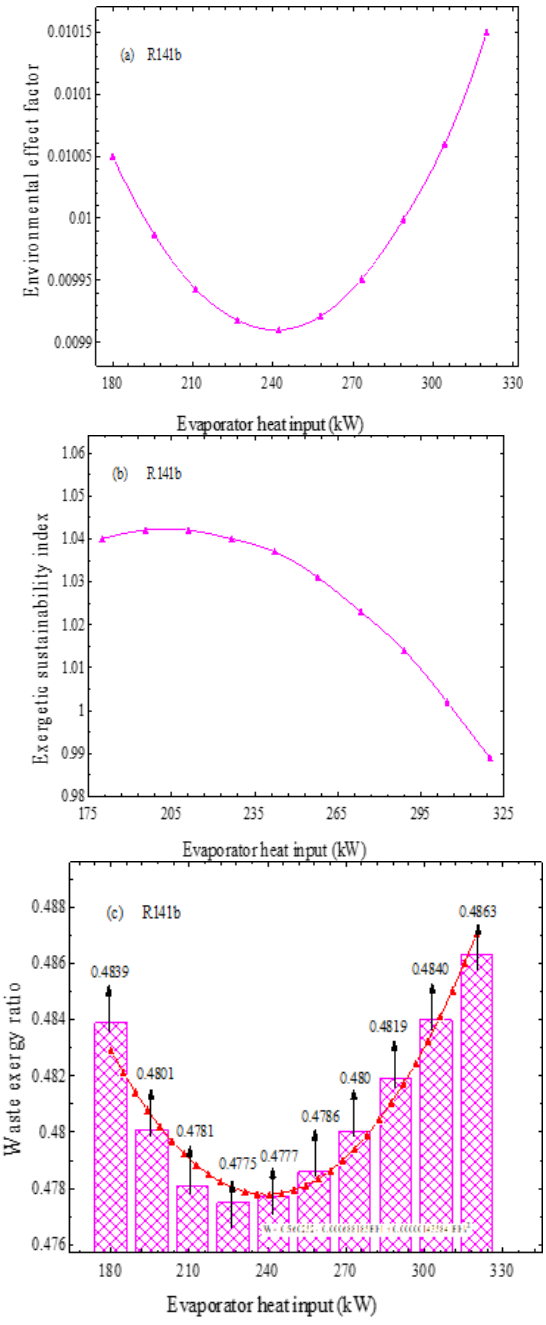

Fig. 8: Effect of EHI on (a) EEF (b) ESI and (c) WER with R114b.

Table 4: Exergy destruction factor at varying evaporator heat input (EHI) with R113 refrigerant.

EHI (kW)	Evaporator	Feed water heater	Heat exchanger	Pump 1	Pump 2	Turbine	Condenser
180.0	0.1101	0.03913	0.0089	2.198E-03	5.047E-03	0.0586	0.3487
195.6	0.1049	0.03892	0.0097	2.080E-03	4.644E-03	0.0572	0.3185
211.1	0.0997	0.03891	0.0103	1.975E-03	4.303E-03	0.0560	0.2930
226.7	0.0943	0.03898	0.0112	1.889E-03	4.007E-03	0.0549	0.2711
242.2	0.0889	0.03913	0.0115	1.796E-03	3.751E-03	0.0539	0.2521
257.8	0.0836	0.03929	0.0115	1.719E-03	3.524E-03	0.0299	0.2355
273.3	0.0782	0.03944	0.0118	1.649E-03	3.324E-03	0.0521	0.2210
288.9	0.0729	0.03960	0.0120	1.584E-03	3.144E-03	0.0513	0.2080
304.4	0.0674	0.03975	0.0121	1.524E-03	2.984E-03	0.0053	0.1965
320.0	0.0645	0.03988	0.0122	1.469E-03	2.839E-03	0.0498	0.1861

Table 5: Exergy destruction factor at varying evaporator heat input (EHI) with R141b refrigerant.

EHI (kW)	Evaporator	Feed water heater	Heat exchanger	Pump 1	Pump 2	Turbine	Condenser
180.0	0.1178	0.03824	0.0013	3.62E-03	8.389E-06	0.06306	0.2427
195.6	0.1165	0.03687	0.0032	3.46E-03	7.720E-06	0.06319	0.2419
211.1	0.1145	0.03613	0.0226	3.31E-03	7.153E-06	0.06319	0.2416
226.7	0.1119	0.03580	0.0039	3.17E-03	6.661E-06	0.06308	0.2416
242.2	0.1089	0.03578	0.0053	3.04E-03	6.235E-06	0.06288	0.2418
257.8	0.1054	0.03593	0.0064	2.93E-03	5.857E-06	0.06261	0.2422
273.3	0.1016	0.03623	0.0074	2.82E-03	5.525E-06	0.06231	0.2427
288.9	0.0976	0.03659	0.0082	2.72E-03	5.227E-06	0.06192	0.2433
304.4	0.0934	0.03699	0.0089	2.63E-03	4.961E-06	0.06160	0.2440
320.0	0.0891	0.03741	0.0095	2.54E-03	4.719E-06	0.06119	0.2447

Table 6: Exergy destruction factor at varying evaporator heat input (EHI) with R245fa refrigerant.

EHI (kW)	Evaporator	Feed water heater	Heat exchanger	Pump 1	Pump 2	Turbine	Condenser
180.0	0.0809	0.09083	0.01389	6.89E-06	7.56E-06	0.05223	0.06411
195.6	0.0748	0.09156	0.01410	6.66E-06	6.95E-06	0.05118	0.07122
211.1	0.0689	0.09223	0.01426	6.44E-06	6.44E-06	0.05026	0.07835
226.7	0.0630	0.09306	0.01438	6.24E-06	5.99E-06	0.04936	0.08540
242.2	0.0574	0.09329	0.01446	6.05E-06	5.62E-06	0.04860	0.09249
257.8	0.0519	0.09329	0.01451	5.87E-06	5.23E-06	0.04787	0.09946
273.3	0.0465	0.09349	0.01454	5.70E-06	4.98E-06	0.04720	0.10640
288.9	0.0413	0.09353	0.01453	5.55E-06	4.71E-06	0.04656	0.11339
304.4	0.0361	0.09356	0.01453	5.54E-06	4.47E-06	0.04596	0.12010
320.0	0.0311	0.09347	0.01450	5.25E-06	4.25E-06	0.04538	0.12670

5.3 Determination of functional sustainability limit (FSL*)*

In determining the functional sustainability limit (FSL) or the exergetic sustainability limit (ESL), the effect of EHI on the exergetic sustainability indicators is considered again. The EEF measures the R245fa performance (Fig.9a) at varying EHI. Between the EEF range, $0.0098 \leq \text{EEF} \leq 0.0095$ and EHI range, $180 \leq \text{EHI} \leq 247.92\,\text{kW}$ the environmental safe limit (ESAL) is evaluated at minimum $\left(\frac{\partial EEF}{\partial EHI} = 0\right)$. From Fig.9a, the ESAL is defined by the coordinate **C** (0.0098, 247.92 kW) while the area ABCD describes the environmental safe operating region which range between $180 \leq \text{EHI} \leq 247.92\,\text{kW}$ and $0.0098 \leq \text{EEF} \leq 0.0095$ for EHI and EEF respectively. Above the EHI of 247.92 kW the potential of R245fa decreases. In (Fig. 9b) the exergetic sustainability index (ESI) increases from about 1.08 at 180 kW to 1.10 at 247.92 kW. At EHI of 247.92 kW which describe the ESAL in (Fig. 9a), this value is approximated in (Fig. 9b) to obtain the ESI. The intersection between the ESI and EHI at coordinate **C** (1.10, 247.92 kW) describes the functional sustainability limit (FSL) or exergetic sustainability limit (ESL) for R245fa. The area ABCD in (Fig. 9b) is the region where the refrigerant will perform optimally. In Fig.10a the ESAL is described by the coordinates C (0.01076, 191.88 kW) while ABCD is the environmental safe operating region defined between $180 \leq \text{EHI} \leq 191.88\,\text{kW}$ and $0.00104 \leq \text{EEF} \leq 0.01076$. The FSL is defined in (Fig. 10b) by coordinates D (0.924, 191.88 kW). The FSL for R113 refrigerant in the considered RORC is 0.924 at EHI of 191.88 kW. Similarly, the ESAL and FSL for R141b are defined in Fig.11a and 11b at C (0.0099, 240 kW) and C (1.035, 240.11kW) respectively. The results show that the FSL varies for different refrigerant possibly it will vary for different cycle configuration. The ozone depleting potential (ODP) of the considered refrigerants is 1.0, 0.11 and 0.0 for R113, R141b and R245fa respectively. Also, the global warming potential (GWP) is 6130, 725 and 950 in same order. Comparing these values with the FSL or ESL obtained from the study, it is clear that R245fa with the highest FSL of 1.10 and least EEF of 0.00958 reflects the ODP and GWP values which exist at 0.0 and 950. The fact that the ODP of R245fa is zero, yet the tendency to affect the environment in a long time as a measure of its GWP still exist. Furthermore, the R113 refrigerant had the highest EEF of 0.01076 and the lowest FSL of 0.924. This is reflected in its ODP value of 1.0 and GWP of 6130. The study indicate that R113 has a low FSL for this reason its ecofriendly potential is low. The latter is evident in the continuous increase in EEF at all EHI in (Fig.10a). Also,

R141b showed a closed performance with R245fa having a good thermal performance, comparable ESI but show high potential to affect the environment. The study establishes that there exists a thermodynamic limit at which a refrigerant can function effectively with less environmental impact based on thermodynamic inputs. Thus, the need for optimization and the design of system to operate on such optimal parameters or sustainability limits will enhanced performance and reduce environmental complications.

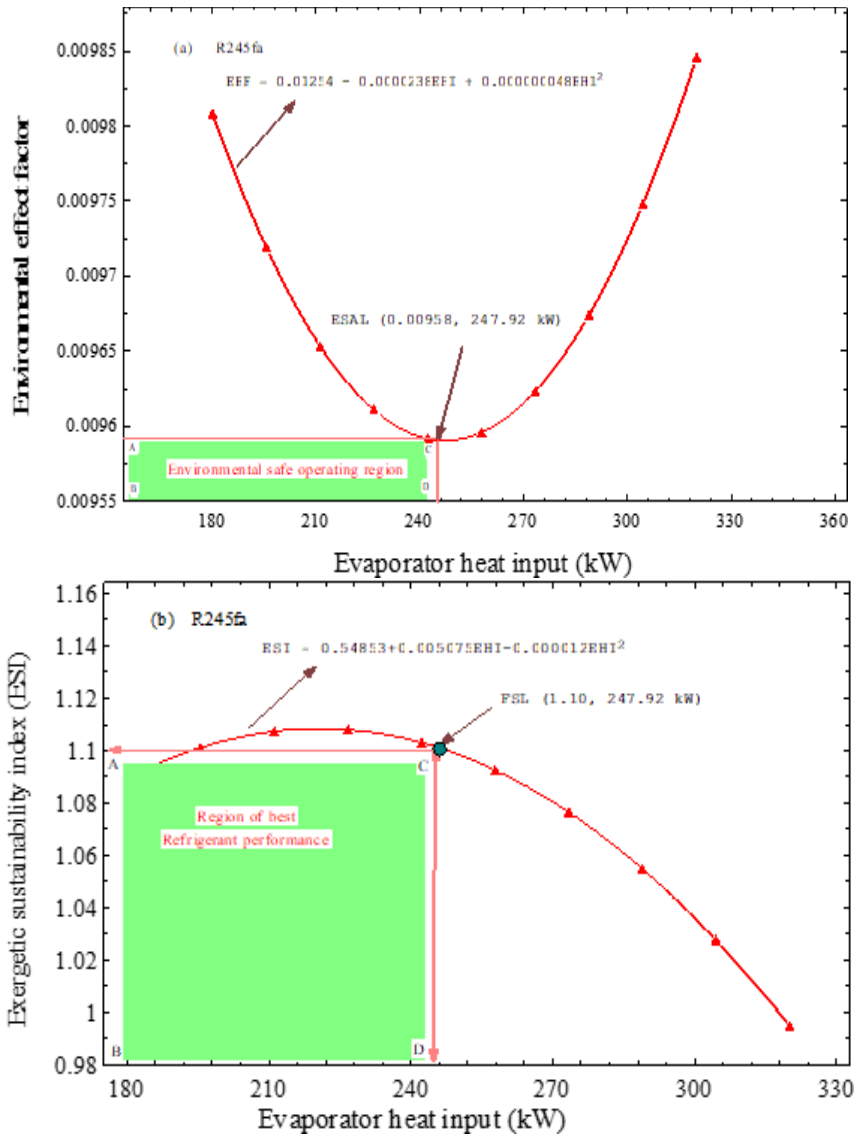

Fig. 9: The effect of EHI with R245fa on (a) environmental effect factor (b) exergetic sustainability index.

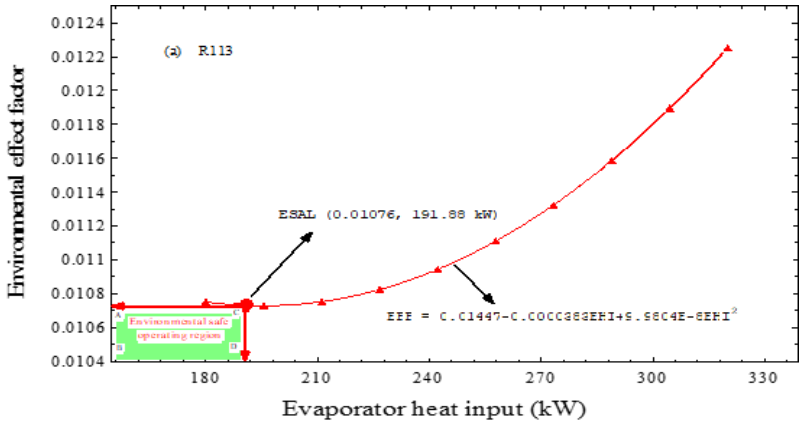

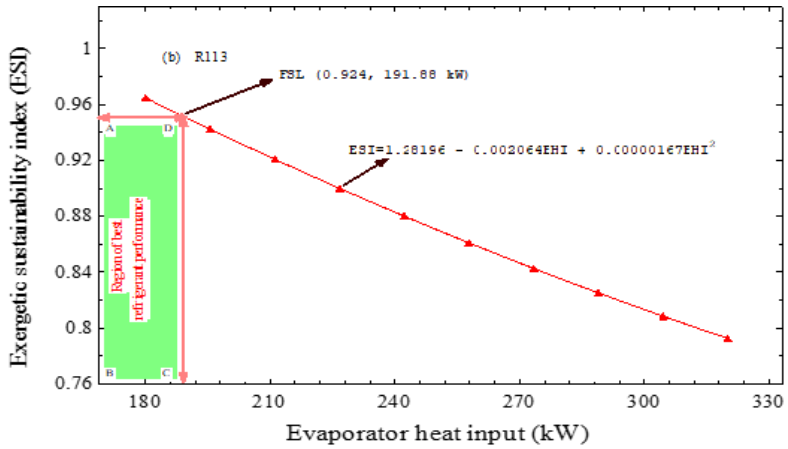

Fig. 10: The effect of EHI with R1113 on (a) environmental effect factor (b) exergetic sustainability index.

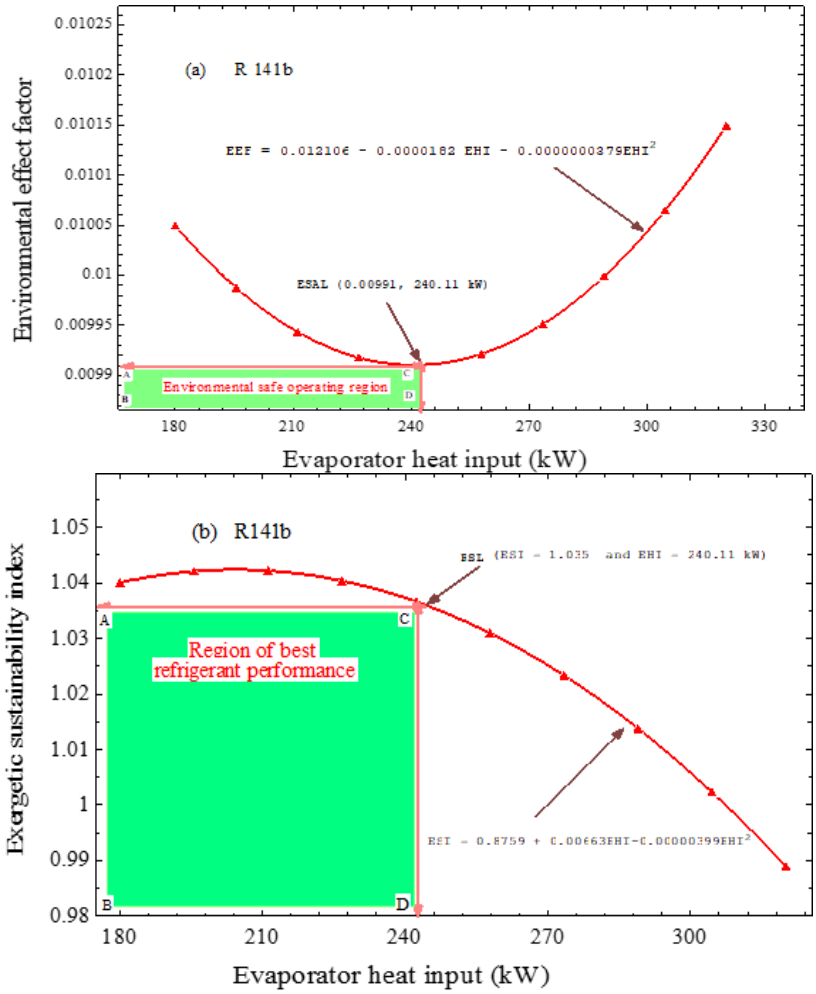

Fig. 11: The effect of EHI with R141 b on (a) environmental effect factor (b) exergetic sustainability index.

6.0 Conclusion

The results of thermal and functional sustainability analysis of a regenerative organic Rankine cycle at different EHI is summarised as follows:

- The overall exergy efficiency and exergy destruction for the RORC with R113, R141b and R245fa refrigerants ranged between 45.64 and 49.24% for EIH variation between $180 \leq EHI \leq 320$ while the turbine power output (TOP) increases with increasing EHI for all the refrigerants. Though OED in the ROCR was high using R245fa while OEF was high with R141b.
- The EEF for R113, R141b, and R245fa ranged between $0.0108 \leq \text{EEF} \leq 0.0122$, $0.01040 \leq \text{EEF} \leq 0.01076$ and $0.0095 \leq \text{EEF} \leq 0.0098$ respectively for EHI range between $180 \leq \text{EHI} \leq 320$ kW. The environmentally safe operating limits for the thermodynamic inputs was found to exist at EHI of 191.88 kW, 240.11kW and 247.92 kW for R113 for R113, R141b and R245fa respectively.
- The internal exergy destruction (IED) or the WER was found to denominate in the RORC using R113. The WER using R113 was about 6.67 % higher than R245fa at 180 kW EHI, 7.12 % higher at 196 kW EHI and 11.03 % higher at 320 kW EHI.
- The functional sustainability limit (FSL) or exergetic sustainability limit (ESL) were determined at 1.10,

1.035 and 0.924 for R245fa, R141b and R113 respectively. The R245fa was found to be more sustainable than other refrigerants.

- The study concludes that optimum sustainable limits of working fluids are important for system design as this will enhance performance and reduce environmental concerns.

References

1. H.Chen, D.Y.Goswami, E.K.Stefanakos, A review of thermodynamic cycles and working fluids for the conversion of low-grade heat, Renew. Sustain. Energy Rev. 14(2010)3059-3067.
2. G. Pei, J. Li, Y. Li, D. Wang, J. Ji. 2011, Construction and dynamic test of a small-organic Rankine cycle, Energy 36 (2011)3215-3223.
3. X.D.Wang, L. Zhao, J.L.Wang, W.Z. Zhang, X.Z. Zhao, W. Wu, Performance evaluation of a low-temperature solar Rankine cycle system utilizing R245fa, Solar Energy 84(2010)353-364
4. H. Kang, Design and experimental study of ORC (Organic Rankine cycle) and radial turbine using R245fa as working fluid, Energy 41(2012) 514-524.
5. A. Marin, A. Dobrovicescu, L. Grosu, A. Gheorghian, Energy and exergy analysis of a combined cooling and power organic Rankine cycle." U.P.B. Sci. Bull. Series D, 76(4) (2014)127-136.
6. D. Scardigno, E. Fanelli, A. Viggiano, G. Braccio, V. Magi, A genetic optimization of a hybrid organic Rankine plant for solar and low-grade energy sources, Energy 91(2015)807-815.
7. A. Algieri, P. Morrone, Comparative energetic analysis of high-temperature subcritical and transcritical Organic Rankine Cycle (ORC), A biomass application in the Sibari district. Appl. Therm. Eng. 36(2012)236-244
8. D. Wang, X. Ling, H. Peng, Performance analysis of double organic Rankine cycle for discontinuous low temperature waste heat recovery. Appl. Therm. Eng. 48(2012)63-71
9. O. Kaska, Energy and exergy analysis of an organic Rankine for power generation from waste heat recovery in steel industry, Energy Convers. Manage. 77(2014)108-117
10. F. Campana, M. Bianchi, L. Branchini, A. De Pascale, A. Peretto, M. Baresi, A. Fermi, N. Rossetti, R. Vescovo, ORC waste heat recovery in European energy-intensive industries: energy and GHG savings. Energy Convers Manage. 76(2013)244-52.
11. T. C. Hung, S. K. Wang, C. H. Kuo, B. S. Pei, K. F. Tsai, A study of organic working fluids on system efficiency of an ORC using low-grade energy sources, Energy, 35(2010) 1403-1411, 2010.
12. K. H. Kim, Effects of superheating on thermodynamic performance of organic Rankine cycles, WASET, 78(2011) 608-612.
13. K. H. Kim, C. H. Han, Analysis of transcritical organic Rankine cycles for low-grade heat conversion," Adv. Sci. Lett. 8(2012) 216-221.
14. K. H. Kim, H. J. Ko. Exegetical performance assessment of organic Rankine cycle with superheating, App. Mech. Materials 234(2012)69-73.
15. H.D.M. Hettiarachchi, M. Golubovic, W.M. Worek, Y. Ikegami, Optimum design criteria for an organic Rankine cycle using low-temperature geothermal heat sources, Energy 32(2007)1698-706.
16. B. Saleh, G. Koglbauer, M. Wedland, J. Fischer. Working fluids for low-temperature organic Rankine cycles. Energy 32(2007)1210-21.
17. H. J. Ko, S. W. Kim, C. H. Han, K. H. Ki, Effects of Source Temperature on Thermodynamic Performance of Transcritical Organic Rankine Cycle. Inter. J. Materials, Mechanics and Manufact. 1(2013)55-59.
18. J.P. Roy, A. Misra, Comparative performance study of different configurations of organic Rankine cycle using low-grade waste heat for Power generation, 2016. Inter. J. Green Energy, DOI:10.1080/15435075.2016.1253570.
19. Mahdi Hatf Kadhum Aboaltabooq, Tudor Prisecaru, Horatiu Pop, Valentin Apostol, Malina Prisecaru, Gheorghe Popescu, Elena Pop, Ana-Maria Alexandru, Cristian Petcu, Cristina Ciobanu, Effect of variable heat input on the heat transfer characteristics in an Organic Rankine Cycle System Renewable Energy Environmental. Sustainability. 1(13) (2016).
20. Chao He, C., Jiao, Y., Tian, C., Wang, Z., Zhang, Z. 2017. The Exergy Loss Distribution and the Heat Transfer Capability in Subcritical Organic Rankine Cycle. Entropy, 19(256) (2017) 256; doi:10.3390/e19060256
21. P. J. Mago, Exergetic Evaluation of an Organic Rankine Cycle Using Medium-Grade Waste Heat, Energy Sources, Part A: Recovery, Utilization, and Environmental Effects, 34(19) (2012)1768- 1780, DOI: 10.1080/15567036.2010.492382.
22. F. I. Abam, E. B. Ekwe, T. A. Briggs, S. O. Effiom, O. S. Ohunakin, M. Allen. Thermodynamic performance and environmental sustainability of adapted organic Rankine cycles at varying evaporator pressure, 2017, Internt. J. Ambient Energy. http://dx.doi.org/10.1080/01430750.2017.130363.
23. Technical Data Sheet of HCFC-141b – Daikin, https://www.chemours.com/Formacel/en_US/products/hcfc_141b.htm, 2017 (accessed 25 September 2017).
24. Refrigerants Environmental Data, www.linde-gas.com/...global...global/.../Refrigerants, 2017 (accessed 25 September 2017).
25. B. F. Tchanche, G. A. Lambrinos, Frangoudakis, G. Papadakis. Exergy analysis of micro-organic Rankine power cycles for a small scale solar driven reverse osmosis desalination system, Appl. Energy 87(2010)1295-1306.
26. Y. Cengel, M. Boles, Thermodynamics an engineering approach. McGraw-Hill, Singapore (2007).
27. S. Safarian, F. Aramoun, Energy and exergy assessments of modified organic Rankine cycles (ORCs), Energy Report, 1(2015)1-7.
28. H. Aydın, T. Önder, T.H. Karako, A. Midilli, Exergo-sustainability indicators of a turboprop aircraft for the phases of a flight, Energy 58 (2013) 550–560.
29. O. Turan, H. Aydin, Exergy-based sustainability analysis of a low-bypass turbofan engine: A case study for JT8D, Energy Procedia 95(2016)499-506, doi: 10.1016/j.egypro.2016.09.075.
30. O. Balli, A. Hepbasli, Exergoeconomic, sustainability and environmental damage cost analysis of T56 turboprop engine, Energy 64(2014)582-600.